International Journal of Signal Processing, Image Processing and Pattern Recognition
Vol.9, No.10, (2016), pp.109-126
http://dx.doi.org/10.14257/ijsip.2016.9.10.11

A Novel Algorithm for Green Citrus Detection based on the Reticulate Grayladder Feature

Mingjun Wang[1,2], Jun Zhou[2], Weiyan Shang[1], Rufu Hu[1], Xuefeng Wang[1] and Liang Gong[3]

[1]*Department of mechanical engineering, Ningbo University of Technology, Ningbo 315016, China*
[2]*Jiangsu key laboratory for intelligent agricultural equipment, Nanjing Agricultural University, Nanjing 210031, China*
[3]*Department of mechanical engineering, Shanghai Jiaotong University, Shanghai 200240*
mjwang1104@126.com

Abstract

Immature green citrus fruit detection using conventional color images is a challenging task due to fruit color similarity with the background, partial occlusion, varying illumination and shape irregularity. Therefore, most existing green fruits detection algorithms, which use color as the main discriminant feature, have a low recognition rate and a high rate of false positives. In this manuscript, we developed a novel Green Citrus fruit Detection algorithm based on the proposed Reticulate Grayladder Feature (GCDRGF), which contained 4 major steps: First, an 8-graylevel image was generated by the preprocessing steps of median filtering, histogram-based equalization and 8-graylevel discretization of the input raw image. Secondly, reticulate grayladders were obtained by a multidirectional scanning on the 8-graylevel image, and rule-based pseudo-grayladder removal strategies were used to remove false positives of target grayladders. Thirdly, grayladder clustering and fruit location fitting were used to generate candidate regions for target fruits. Finally, majority voting was performed to determine the results of candidate regions based on the analysis of apparent features and recticulate grayladders within candidate regions. The experimental results proved the effectiveness of the proposed reticulate grayladder feature and the corresponding detection algorithm with respect to various illuminant and imaging conditions. Compared with the existed eigenfruit algorithm, our algorithm has a higher rate of successful recognition and a lower rate of false positives, which helps to greatly improve the productivity of robotic operations.

Keywords: *reticulate grayladder features, green citrus detection, image segmentation*

1. Introduction

Recognition of immature fruit on trees is an important and still challenging issue in agriculture, which has potential applications ranging from robotic harvesting to fruit load estimation and yield forecasting. One of the major challenges in detecting immature green citrus fruit lies in the similarity of the colour of the fruit and the leaves [1]. And non-uniform illumination is another challenging problem, since the vision-based recognition algorithm has to work under natural outdoor conditions. Furthermore,

ISSN: 2005-4254 IJSIP

fruit shape irregularity and partial occlusion of the fruit by leaves, branches and by other fruits can also cause challenges in detecting green fruits using computer vision.

While most of existing studies aimed at detecting mature fruits [2-8], researchers started investigating immature fruit detection earlier in this century [1] and [9-12]. Kane and Lee [9] used multi-spectral imaging, and developed an image processing system based on pixel classification for green citrus detection. Using an NIR camera, they captured images at different wavelengths and carried out an index calculation method to merge those images. They could successfully classify 84.5% of the fruit pixels using multi-spectral imaging. Hiroshi [10] proposed a green citrus detection algorithm using hyperspectral imaging. First, a pixel discrimination function was generated based upon a linear discriminant analysis and applied to all pixels in a hyperspectral image for image segmentation of fruit and other objects. Then, spatial image processing steps (noise reduction filtering, labeling, and area thresholding) were applied to the segmented image, and green citrus fruits were detected. The results of pixel identification tests showed that detection success rates were 70-85%, depending on citrus varieties. Stajnko, Lakota, and Hocevar[11] used images captured by a thermal camera to estimate the number of apples and measured their diameter. Thermography (sensing the heat radiation on an object) and several image processing algorithms were employed in their approach.

However, most of these studies investigated green fruits detection using multi-spectral, hyperspectral and thermal imaging techniques, which used high-priced equipment. It is necessary to develop a more affordable method for immature green fruits detection using conventional color images [13]. Si Yongsheng [14] proposed an apple recognition method based on K-means algorithm, which used both color feature and texture features to recognize the object. The experimental results showed that the apple fruits could be recognized successfully in various conditions. The recognition rate reached 81%. The algorithm proposed by Raphael [15] included four main steps: detection of pixels that have a high probability of belonging to apples, using color and smoothness; formation and extension of "seed areas", which are connected sets of pixels that have a high probability of belonging to apples; segmentation of the contours of these seed areas into arcs and amorphous segments; and combination of these arcs and comparison of the resulting circle with a simple model of an apple. The experimental results showed that 85% of the apples were detected successfully. Kurtulmus [13] developed a machine vision algorithm to detect and count immature green citrus fruits in natural canopies using color images. Color, circular Gabor texture analysis and a novel ‘eigenfruit’ approach were used for green citrus detection. A shifting sub-window at three different scales was used to scan the entire image for finding the green fruits. Each sub-window was classified three times by eigenfruit approach using intensity component, eigenfruit approach using saturation component, and circular Gabor texture. Majority voting was performed to determine the results of the subwindow classifiers. Blob analysis was performed to merge multiple detections for the same fruit. For the validation set, 75.3% of the actual fruits were successfully detected using the proposed algorithm.

However, these green fruits detection algorithms generally used color as the main discriminant feature, which can be easily affected by illumination changes. As a result, they had a low recognition rate and a high rate of false positives. Therefore, it is necessary to design a new detection algorithm using a certain illumination-insensitive feature as the main feature.

In this paper, we developed a novel green citrus fruit detection algorithm based on the reticulate grayladder feature(GCDRGF). The novelty of our method lies in 2 aspects: 1. The reticulate grayladder feature was proposed and used as the main discriminant feature instead of the color feature in existed algorithms. The reticulate grayladder feature depicted the complete graylevel shift of local fruits' surface, which was generally independent of illumination changes and improved robustness of proposed algorithms under various conditions. 2. We designed a two-level mechanism for pseudo-targets removal. In details, scaling differences between target fruits and other entities on trees were integrated in the pseudo-grayladder removal rules. Furthermore, statistical characteristics of reticulate grayladders and apparent features of fruits' regions were fused in majority voting to further remove pseudo-fruits.

2. Material and Algorithm

2.1. Image Acquisition

For developing and testing proposed algorithm, images were acquired in the natural daylight illumination conditions(both sunny and cloudy) using a typical digital camera (IMX214, Sony) with a resolution of 4160 x 2336 pixels from citrus trees. At the green stage of the immature citrus fruits, a total of 186 images(114 images for sunny scenes, and 72 for cloudy days) were taken at various times in October 2014 from an experimental citrus grove in the city of Ningbo, China. 1/3 of 186 images were used for parameter training, others were used as validation dataset. Image samples were then randomly cropped and resized to 512 x 384 pixels for computational convenience. For resizing images, a bicubic interpolation method was used in this study. Fruits in most images have various degrees of shadow, occlusions and fruit overlap. And it was random that a certain fruit was in shadow side or sunny side. The imaging range of the actual scene of the captured images was approximately 20 to 60 cm.

In our implementation, all algorithms and experiments were performed on MATLAB version 7.14.0.739 (R2010a) with a 64-Bit Intel_ Core i7-3520M 2.90 GHz CPU. The main purpose of this study was to demonstrate the concept of the reticulate grayladder feature and validate the effectiveness of the corresponding detection algorithm. We leave the real-time algorithm implementation for future study in order to incorprate the algorithm in final algricultural robots.

2.2. Overview of the Proposed Algorithm

The flowchart of the main algorithm is shown in

Figure **1**. First, an 8-graylevel image was generated by prepocessing steps(section 2.3) of median filtering, histogram-based equalization and 8-graylevel discretization of the input raw image. Secondly, reticulate grayladders were obtained by a multidirectional scanning on the 8-graylevel image(section 2.4), and rule-based pseudo-grayladder removal strategies(section 2.5) were used to remove false positives of target grayladders. Thirdly, grayladder clustering and fruit location fitting were used to generate candidate regions for target fruits(section 2.6). Finally, majority voting(section 2.7) was performed to determine the sesults of candidate regions based on the analysis of apparent features and recticulate grayladders within candidate regions.

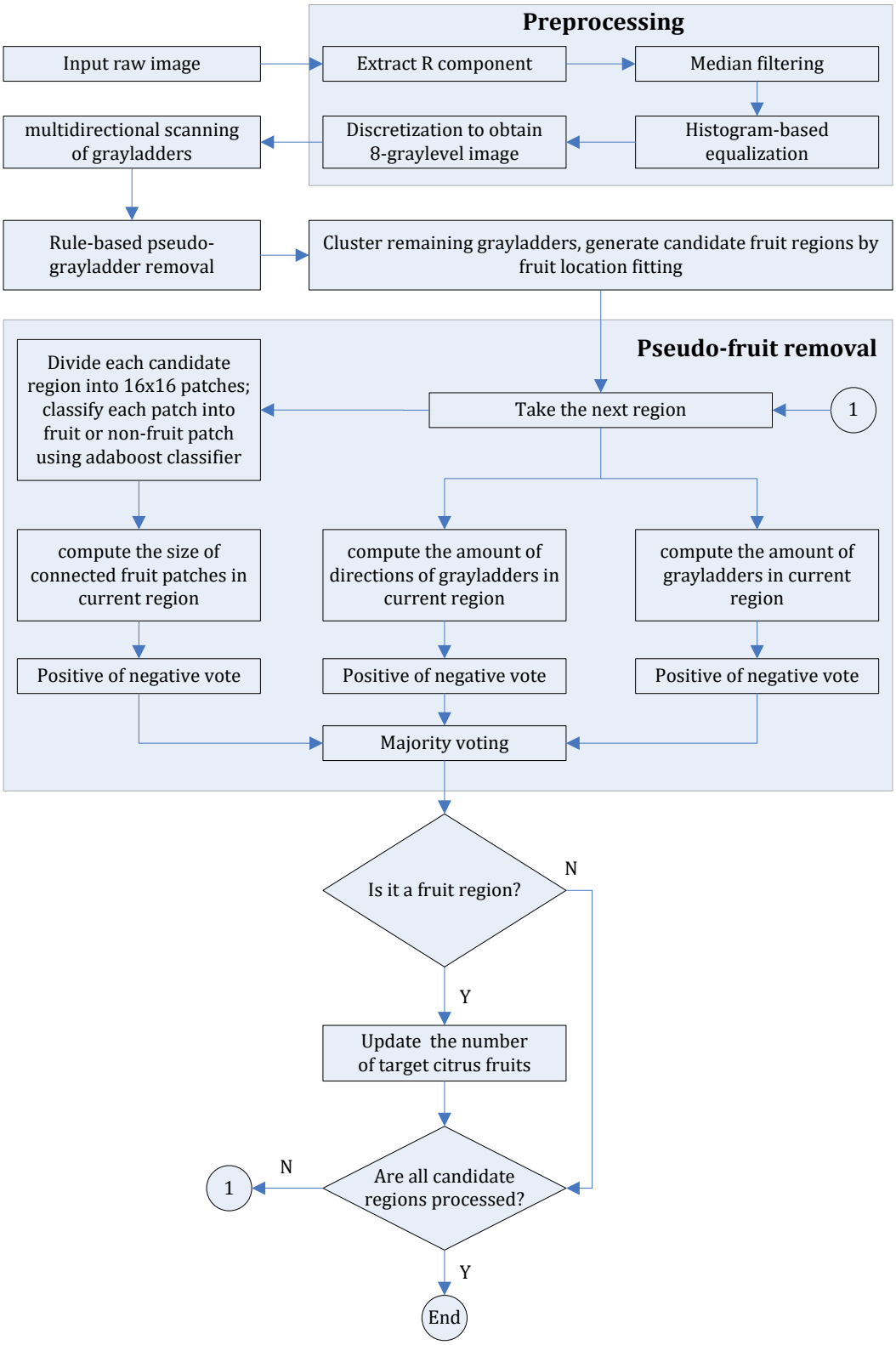

Figure 1. Flowchart of the Proposed Green Citrus Detection Algorithm

2.3. Preprocessing

The preprocessing of the image is shown in Figure 2, which mainly consists of 3 steps. First, the R component of the raw image was extracted and median filtered to reduce noise. Secondly, histogram-based equalization was used to improve the contrast of the image. Thirdly, the resulting image was further discretized to obtain 8-graylevel superpixel expression of the original scene as shown in Figure 2(d).

2.4. Multidirectional Scanning of Grayladders

As shown in Figure 2(d), the graylevel of fruit surface gradually dicreases from the center to edge because of the reflection characteristics of a spheriod (the fruit can be treated as a spheriod proximately). We defined the terrace-shaped graylevel distribution of fruit surface as graylevel terrace, and the graylevel decreasing sequence(a complete graylevel shift) with respect to a certain direction was defined as a grayladder. It is difficult to find a proper descriptor for the graylevel terrace. Instead, we used multidirectional grayladders(reticulate grayladders) as the main feature to detect green citrus fruits.

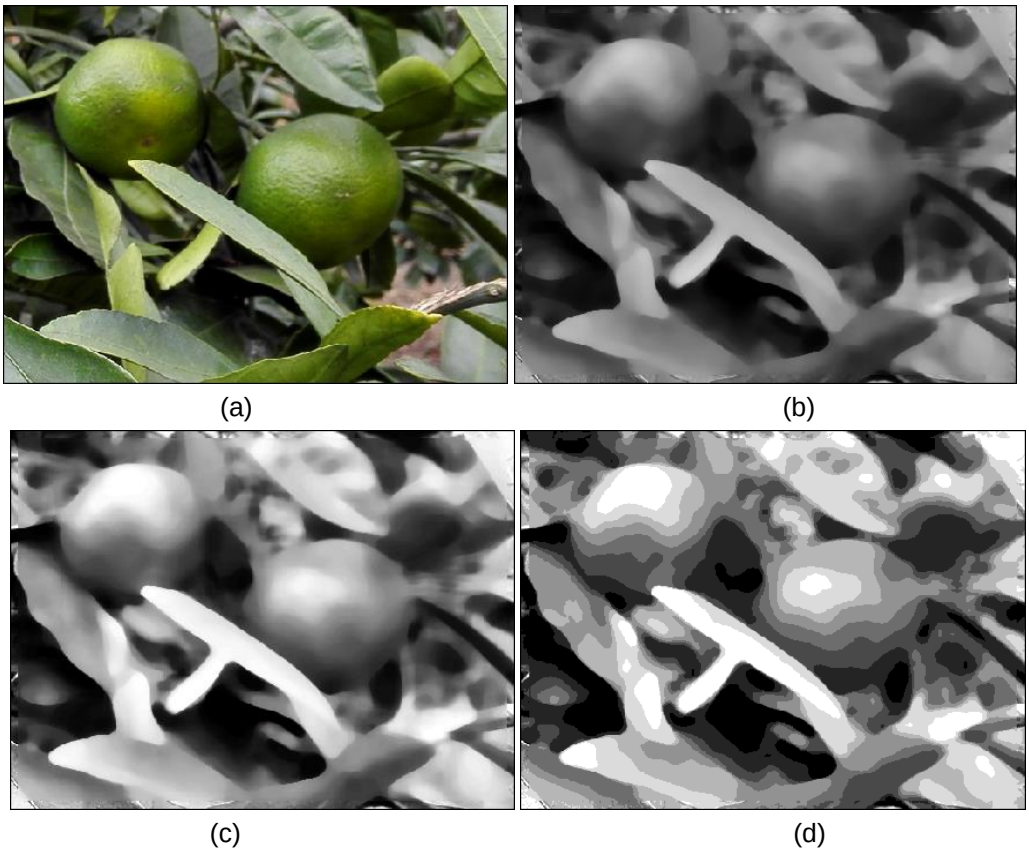

Figure 2. Preprocessing of the Image, (a) Raw Image, (b) Median Filtering Output of R Component Image, (c) Histogram-Based Equalization Output, (d) 8-Graylevel Discretization Result

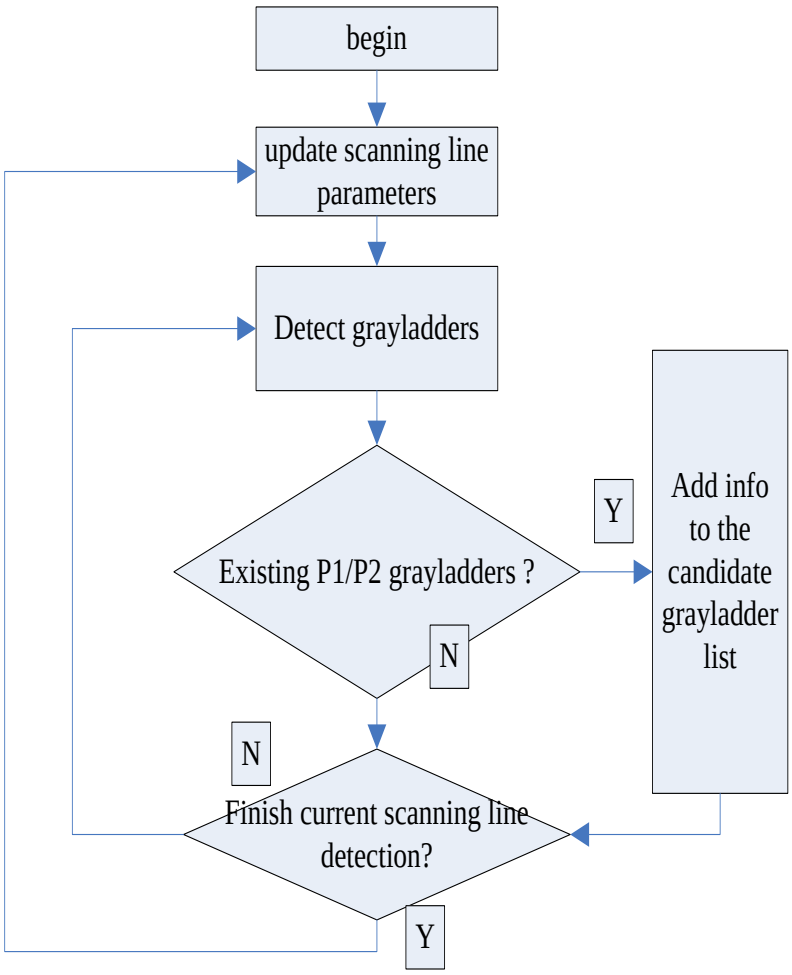

Figure 3. Flowchart of the Multidirectional Grayladder Scanning Process

The flowchart of the scanning process is shown in Figure 3. The main steps contain:

(a) Determine or update parameters of the current scan line, which consists of the scan angle and the start point. The scan angle is the angle between the scanning direction and the horizontal x-axis. Only grayladders having angles of [0,180] are scanned with an interval of 15 degree. The start point of a scan line lies on the edges of an image, and the horizontal interval between different start points is 10 pixels.

(b) Detect a specific graylevel sequence(grayladder) of the current scan line. If it exists, add the corresponding information to the candidate grayladder list. There are 4 kinds of candidate grayladders, which are 87654321, 8765432, 7654321, and 765432 sequences respectively. Most sequences start from '8', and some fruits in shadow side begin from '7'. We name the fromer pattern1(P1) and the latter pattern2(P2).

(c) Check if the detection on the current scan line is completed? If not, continue to detect. If yes, go to the step of (a) to start another new scan line.

Scanning results of 6 randomly selected images were shown in Figure 4, the grayladders were represented as white line segments. As indicated by Figure 4, reticulate grayladders lay on the fruit surface and each grayladder originated on the highest-graylevel superpixel and

ran through several superpixels of different graylevels in a descending order. There also existed lots of pseudo-grayladders outside fruit surface regions, which can be divided into 3 categories: pseudo-grayladders generated by branch surfaces, by leaf surfaces and by random scene geometry. It is necessary to remove these 3 kinds of pseudo-grayladders.

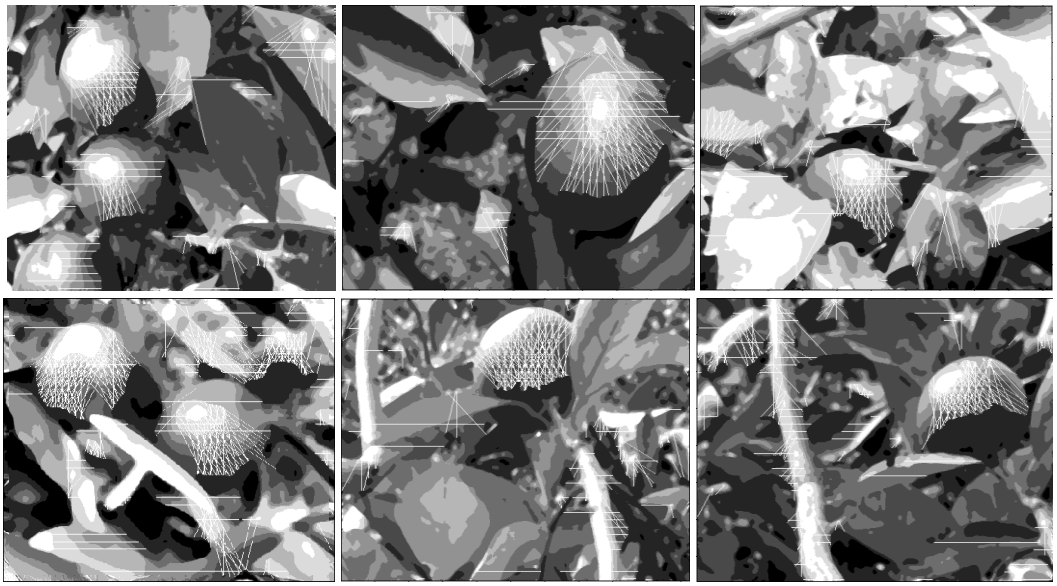

Figure 4. Initial Scanning Results of Grayladders for Typical Scenes

2.5. Rule-Based Pseudo-Grayladders Removal

We first define the concepts of stepwidth and span. As mentioned above, a typical P1 sequence (grayladder) can be represented as follow:

88...877....766.....65...44.....433....322....211.....1

which contains all the graylevels from '8' to '1'. The stepwidth of graylevel i is defined as the length of graylevel i in the sequence. And the length of the whole sequence is defined as the span of the grayladder:

$$sp = \sum_{i} w(i)$$

RULE 1 is used to remove the pseudo-grayladders generated by branch surface, and is defined as

$$vote(1) = \begin{cases} 1, & if\ sp >= k_1 * sp_{low} \\ 0, & if\ sp < k_1 * sp_{low} \end{cases}$$

Which constrains that the span of target (real) grayladders must have a value bigger than $k_1 * sp_{low}$, sp_{low} is the lower limit of the target span, and k_1 is a scale coefficient correlated with the imaging distance and fruit size.

RULE 2 is used to further remove the pseudo-grayladders generated by leaf surface, and is defined as

$$vote(2)=\begin{cases}1, & if \min\limits_{i\neq j}[(w(i)+w(j))/sp]\geq R_{low}\\ 0, & if \min\limits_{i\neq j}[(w(i)+w(j))/sp]<R_{low}\end{cases}$$

Which constrains that, the ratio of two minimum stepwidth in the whole span must be larger than R_{low}.

RULE 3,4,5 are used to filter the pseudo-grayladders generated by the random scene geometry, and are defined respectively as:

$$vote(3)=\begin{cases}1, & if\ sp<=k_1*sp_{high}\\ 0, & if\ sp>k_1*sp_{high}\end{cases}$$

$$vote(4)=\begin{cases}0, & if\ (A>A_{th}*k_1)\bigcap(A/(L^2)\geq R_{high})\\ 1, & else\end{cases}$$

$$vote(5)=\begin{cases}1, & if\ S_{stais}\geq S_{low}\\ 0, & else\end{cases}$$

RULE 3 constrains that the span of target grayladders must have a value smaller than k_1*sp_{high}, sp_{high} is the upper limit of target span, and k_1 is a scale coefficient correlated with the imaging distance and fruit size.

RULE 4 constrains that if the area (A) of highest-graylevel superpixel is bigger than a certain value ($A_{th}*k_1$), the ratio of A and L^2 must be larger than R_{high}. L is the long edge of bounding rectangle of the highest-graylevel superpixel related to the current grayladder. R_{high} is the threshold ratio.

RULE 5 constrains that the number (S_{stais}) of target grayladders correlated with the highest-graylevel superpixel should be bigger than a certain value (S_{low}).

The final discriminant for target grayladders is the ‘AND’ of all the rules above:

$$vote=vote(1)\bigcap vote(2)\bigcap vote(3)\bigcap vote(4)\bigcap vote(5)$$

Which indicats that, if one of the rules above is not satisfied, the corresponding grayladder will be removed.

Three instances of pseudo-grayladder removal are randomly selected and shown in Figure 5, with parameters sp_{low}, sp_{high}, A_{th}, R_{low}, S_{slow}, R_{high} are set to 40, 130, 500(pixels), 0.18, 3 and 0.25 respectively. k_1 is fixed to 1 and the adaptive adjusting of k_1 with respect to imaging conditions is left to future study.

The results in Figure 5, indicated that, the rules are slightly harsh that some of the real (target) grayladders are removed as shown in Figure 5(f). However, harsh rules contribute to the removing of most pseudo-grayladders and the remaining target grayladders after removal are generally adequate for the following determination of most fruits.

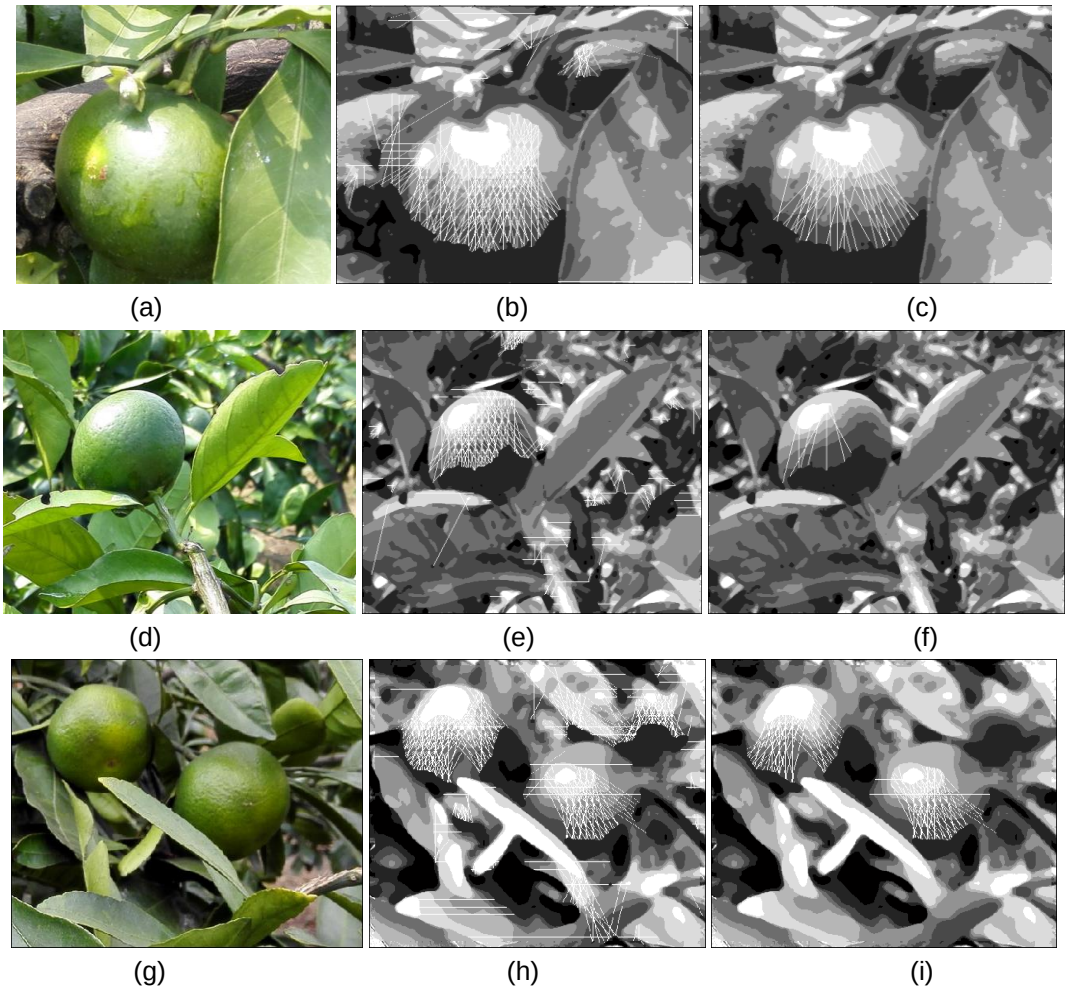

Figure 5. Illustrations of Grayladder Removal: Original Scenes(Left Colunm), Initial Scanning Results(Middle Column), and Rule-Based Removing Results(Right Column)

2.6. Candidate Fruit Region Generation

An ideal fruit scene after pseudo-grayladder removal is shown in Figure 5(i): there is no pseudo- grayladder outside fruit regions and, within the region of each actual fruit, a set of reculate grayladders(grayladder cluster) lie on a certain set of superpixels and each grayladder originates from the highest-graylevel superpixel. However, various random factors (such as local defects of fruit surfaces, partial occlusions caused by carpopodiums or shoots) tend to produce more than one set of grayladders within the same fruit region(multi-detections of the same fruit) and to generate unexpected pseudo-grayladders outside the fruit range(which are similar to target grayladders in scales and can not be completely removed by aforementioned rule-based strategies).

Therefore, we clustered the remaining grayladders to merge multi-detections of the same fruit(steps 1-2) and fitted fruit locations(steps 3-6) to generate candidate fruit regions. The candidate fruit regions contained both actual-fruit-related regions and pseudo-fruit regions caused by aforementioned pseudo-grayladders. And the pseudo-fruit regions(or pseudo-fruits)

will be further eliminated by the subsequent majortity voting step. The detaled steps of candidate fruit region generation is shown as follows:

Step1: Classify grayladders lying on the same set of superpixels into one initial cluster. And K intinal clusters (c_i , $i=1,2...K$) are created accordingly. The data related to each cluster are: a set of grayladders included in the cluster, a counting value n_i representing the amount of grayladders, a set of superpixels($sp_1, sp_2, ...sp_M$), coordinates x_i representing the center of gravity of all superpixels in the set.

Step2: Reorder initial clusters in descending order of n_i , and reconsider each cluster: for the cluster c_j , if c_k , $k = j+1, j+2, ..., K$ satisfies the inequality of $\left|x_j - x_k\right| \le sp_{high}$, and the amount of superpixels corresponding to both c_k and c_j is bigger than 3, then c_k is merged into the cluster c_j . The counting value is updated as $n_{j,new} = n_j + n_k$, and x_j remains the same.

Step3: Again reconsider all initial grayladder clusters successively. For c_i ,compute external rectangulars of all superpixels in the corresponding cluster, and reorder the superpixels in descending order of the rectangular size. The new sorted superpixel sequence is $sp_{1new}, sp_{2new}, ...sp_{Mnew}$.

Step4: Weights of the pixels inside sp_{jnew} are set to be j , which indicates the relative importance of pixels in the following fruit-location fitting operation. The higher the weight of a pixel, the more important it is.

Step5: Circles are used to fit the proximate location of a fruit, whose parameters contains the coordinates of the circle center and the radius. Two factors are taken into account during the fitting step. First, the sum of weights of pixels contained in the circle should be as big as possible. And meanwhile, the circle shouldn't occupy the range outside that of the real fruit. The objective function adopted by the fitting step is:

$$\{x_0, y_0, r_0\} = \arg\max_{x,y,r} \sum_i w_i - k \cdot \exp(r/R) \text{ , } \forall (x_i, y_i) \in \sqrt{(x_i - x)^2 + (y_i - y)^2} \le r$$

$\sum_i w_i$ is the weighting term, which represents the sum of weights of pixels (x_i, y_i) contained in the circle. And $k \cdot \exp(r/R)$ is the penalty term, which indicates that the larger the radius r is, the punishment bigger. k is a coefficient to describe the relative importance of two terms.

Step6: Caculate the value of the objective function with respect to various value combinations of $\{x, y, r\}$, the optimal values x_0 , y_0 and r_0 are obtained when the value of the objective function reaches the biggest.

2.7. Pseudo-Fruit Removal by Majortity Voting

The pseudo-fruit regions(or pseudo-fruits) are further eliminated by majortity voting, which fused 3 aspects of cues to determine whether a candidate region is fruit region or not: a) the apparent features of pixels within the region, b) the amount of grayladders

contained in the candidate region, and c) the amount of directions of grayladders contained in the candidate region.

The apparent features are integrated by the adaboost model [16] and blob analysis. The main steps consists of: 1) divide each candidate fruit region into 16x16 patches and extract apparent features of each patch. The dimension of all apprarent features is 65, which contains means of RGB and R-B, texture descriptors [14], and respective histograms of RGB components. 2) compute the probability of being fruit patchs based on adaboost model. In Figure 6(c), and Figure 6(g), the graylevel of each patch represents the probability of being a fruit patch. The higher patch graylevel is, the more probable it is a fruit patch. 3) separate all patches into two groups by thresholding: fruit patch(probability>0.5) and non-fruit patch(probability<=0.5). White patches in Figure 6(d), and Figure 6(h), represent fruit patches and black patches correspond to non-fruit patches. 4) A positive voting will be made if the blob of connected fruit patches occupies more than 1/3 of the size of current candidate region such as the circles in solid lines in Figure 6(d), and Figure 6(h). Otherwise, a negative voting will be made such as the circle in dashed line in Figure 6(h).

The fusion of the amount and direction of grayladders is a direct process. A positive voting will be made if the amount of grayladders after removal exceeds 6, and another positive voting will be made if the amount of directions of grayladders exceeds 3. Two positive votes are enough for the determination of a target fruit region.

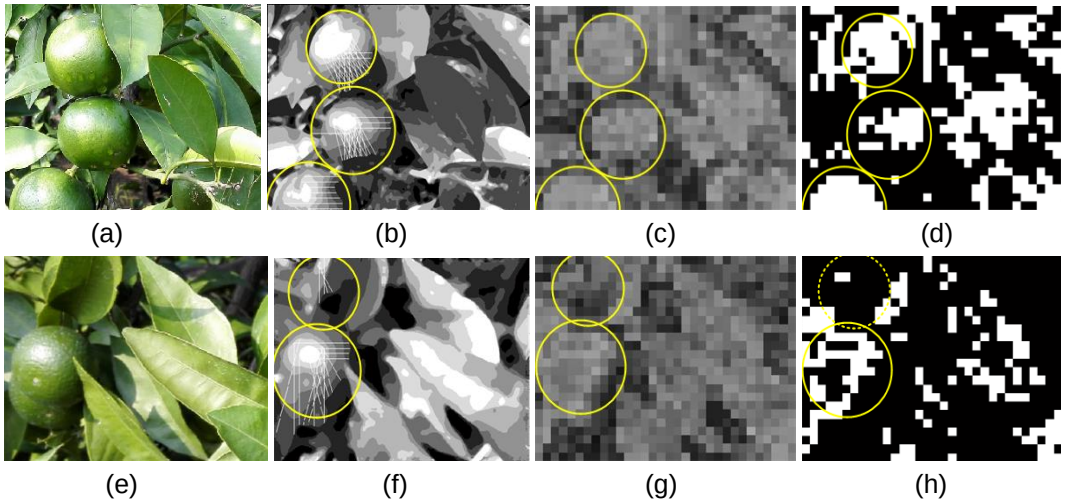

Figure 6. Pseudo-Fruits Removal: (a)(e) Original Images, (b)(f) Candidate Fruit Regions after Clustering and Fruit Location Fitting, (c) (g) Probability of Being Fruit Patch, (d)(h) Grouping Results of Patches by Thresholding

3. Results and Discussions

3.1. Qualitative Results

In Figure 7, three scenes of various imaging conditions were listed (sunny, partial occlusion and cloudy). The left column of Figure 7, contains original scenes and the images of right column indicate the final grayladder sets after removal and the detected fuirts(represented by circles).

Figure 7(a), and Figure 7(b), are used to investigate the effectiveness of reticulate grayladder features under sunny illuminant conditions. The scene of Figure 7(a), contains 3 fruits under sunny illuminant condition. And each fruit surface region can be divided into three categories according to the light-reflection characteristic: high-light areas (this area loses original fruit color due to the specular reflection of oil cells on the surface of fruits), diffuse-reflection areas (diffuse reflection is dominant in this area and the original fruit color is kept), and shadow areas (this area is in the shadow side of the fruit). Results from Figure 7(b), proved the effectiveness of the proposed grayladder. In details, each fruit region contains one and only one set of grayladders, which successively experienced from the highest-graylevel superpixel to the lowest one. The fact that all 3 kinds of aforementioned areas contribute to the generation of grayladders indicates the suitability of grayladder features to the recognition of green citrus fruits, while most existing algorithms in this domain tend to fail when the fruit region contains both the high-light area and the shadow area [17].

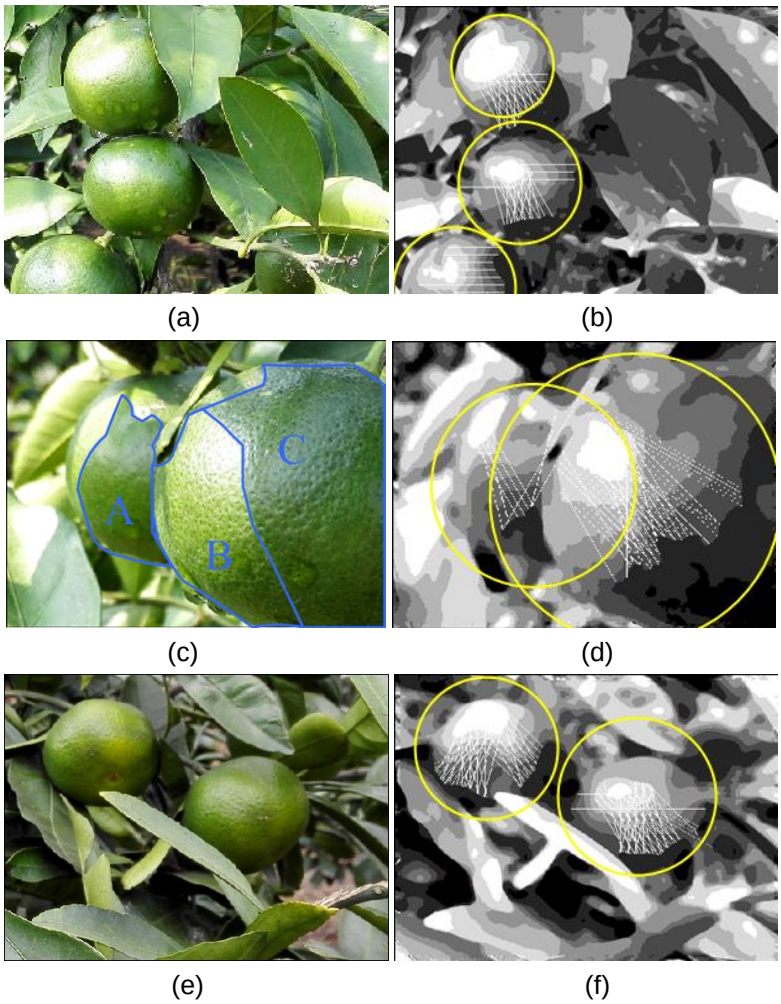

Figure 7. Green Citrus Recognition Results under Various Imaging Conditions: (a)(b) a Sunny Scene with Small Occlusion and Shadow, (c)(d) a Sunny Scene with Big Shadow and Partial Occlusion Caused by Another Fruit, (e)(f) a Cloudy Scene with Little Occlusion and Shadow

Figure 7(c), and Figure 7(d), are used to investigate the influence of shadow and partial occlusion on reticulate grayladder features and the proposed algorithm. Shadow is one of the major obstacles for the recognition of fruits on tree. Consider the scene of Figure 7(c), which contains two fruits: the closer one with half surface in shadow and the back one, whose surface is tatolly covered by highlight, shadow and occluded by the closer fruit. Figure 7(d), shows that the shadow did change the overall graylevel distribution of each fruit region. However, for each local patch on fruits' surface(such as patches A, B and C in Figure 7(c), respectively), part of the graylevel shift is generally maintained inside each patch, as shown in Figure 7(d). And therefore, it is a high probability event that a complete graylevel shift and the corresponding grayladder can be detected when several local patches under different illumination conditions are simultaneously discretized to form an 8-graylevel superpixel image. Partial occlusion is another obstacle for the recognition of fruits on tree. However, Figure 7(d), shows that even when more than 1/2 surface is occluded, the back fruit can still be recognized using the grayladder feature. Our subsequent experimental results show that, in the extreme case when 70% of a fruit surface is occluded, the grayladder can be detected if the fruit is not totally covered by the shadow.

Figure 7(e), and Figure 7(f), are used to investigate the effectiveness of grayladder features under cloudy illuminant conditions. There is no local high-light region on the surface of fruits in Figure 7(e), and the fruits maintain its original color since diffuse-reflection is dominant. Figure 7(f), shows that, fruits under cloudy condition exhibits similar grayladder sets as the ones in Figure 7(b). Graylevels of fruit region are shifted to high graylevel range through the histogram-based equalization operation, which makes the grayladder feature suitable for the fruits under cloudy condition. And two fruits under cloudy condition are successfully detected although they have totally different apparent features from the fruits in sunny illuminant condition, which further indicates the effectiveness and the robustness of the proposed feature and algorithm.

More qualitative recognition results of green citrus scenes were listed in **Figure 8**. Fruits under different kinds of shadow and occlusions were generally recognized except the fruit represented by the dashed circle in **Figure 8**(h). The corresponding fruit is not detected because it lies in the lowest-graylevel region of the whole scene(the fruit is under a complete shadow). In our future study, we plan to develop subwindow-based detection methods to reduce the influence of other high-graylevel regions on the low-graylevel region in the same image.

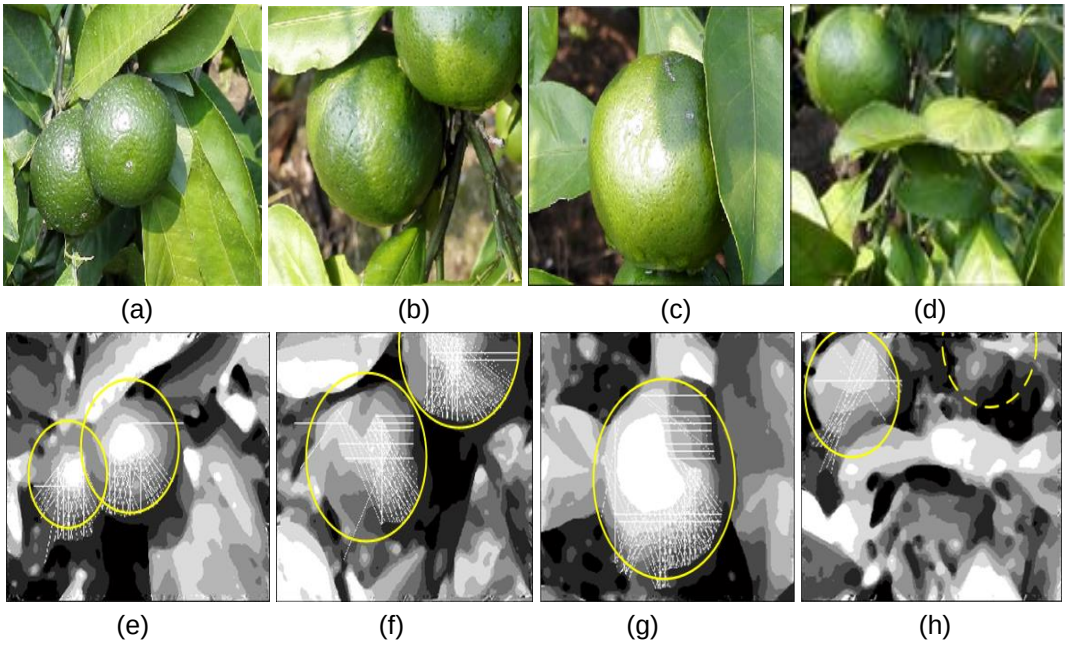

Figure 8. More Qualitative Recognition Results of Scenes

3.2. Quantitative Results

Intermediate results of 25 randomly selected images were listed in **Table 1**. And the first 15 images correspond to the sunny illuminant condition and the last 10 images relate to the cloudy illuminant condition.

Data in **Table 1** show that: for all 25 images, (a) 6671 grayladders were obtained by initial scanning, and 5215 grayladders were removed by 5 rules(most of the removed grayladders were pseudo-grayladders and a small part were target grayladders); (b) 3389 and 1094 grayladders were removed by rule 1 and rule 2 respectively, which accouts for 86% of all the grayladders removed. Therefore, it can be concluded that the main differences between pseudo-grayladders and target grayladders are the span and the stepwidth distribution. Pseudo-grayladders usually have smaller spans and more randomly distributed stepwidths compared with target grayladders.

The remaining 1456 grayladders after pseudo-grayladder removal generated 69 initial grayladder clusters. And the clustering and pseudo-fruit removal steps further eliminated 21 and 7 clusters respectively, which totally reduced potential fruits by 40.6%.

In details, most of the eliminated 28 clusters can be divided to 3 kinds of situations: repetitive-detections due to multiple highest-graylevel superpixels in the same fruit region, repetitive-detections due to simultaneous existence of P1 and P2 grayladder clusters, and randomly generated grayladders and corresponding clusters, which do not correspond to actual fruits.

There are 40 actual green citrus fruits in the 25 images in all. 32 fruits were correctly identified, 8 were missed and 5 false positives were generated. The direct reason for missed fruits is that the fruit region didn't exhibit grayladder clusters of the expected scale. And the indirect reasons are: back fruits almost completely occluded by the closer one(2 fruits), the fruit in complete shadow lay in the lowest graylevel range of the current scene(1 fruit), and various kinds of random factors making grayladders

incomplete(5 fruits). The direct reason for false positives was that non-fruit surfaces exhibited grayladder clusters of the expected scale, which contained two situations: leave surface of specific curvature(4 positives) and branch surface of specific curvature(1 positive).

In order to further evaluate the proposed GCDRGF algorithm, the algorithm of eigenfruit [13] was also implemented and tested using our dataset. Part of experimental results were listed in **Table 2**, which indicates that:

(a) The overall recognition rate of GCDRGF was 80.9%, with 81.97% and 79.22% for sunny and cloudy conditions respectively, which preliminarily proved the effectiveness of GCDRGF algorithm and showed the possibility of green citrus detection using the proposed reticulate grayladder feature based on regular color images.

(b) Totally 19.1% of real fruits under both conditions were not detected. In details, 26.32% of missed fruits couldn't be detected due to mutual fruit occlusion, 13.16% due to the complete shadow on fruits, and others due to various random factors, which resulted in the incomplete or shortage of grayladders. In future study, edge features such as canny can be combined with the proposed reticulate grayladder feature to further improve the recognition rate and reduce false positives.

(c) Compared with eigenfruit algorithm, GCDRGF had a higher rate of successful recognition and a lower rate of false positives. Eigenfruit used color as one of major discriminant features, which was easily affected by illumination changes. Therefore, Eigenfruit detected more false positives in highly-contrasted regions (such as the sunny side of the canopy) than other regions(such as the shadow side of the canopy). However, the proposed GCDRGF used the grayladder as the major feature, which integrated the complete graylevel shift of local fruits' surface and was independent of illumination changes. Therefore, the recognition rates for fruits in both sides of the canopy had no statistical difference(82.09% and 81.82% respectively for sunny and shadow side of the canopy).

Table 1. Results of Green Citrus Recognition

Image	Number of grayladders							Number of grayladder clusters			Recognition result			
	Initial scanning	removed by rule.1	removed by rule.2	removed by rule.3	removed by rule.4	removed by rule.5	remaining	Initial clusters	After Merging	After pseudo-fruit removal	Fruit count	Correctly identified	False positive	missed
1	277	143	45	1	10	11	67	4	3	3	3	3	0	0
2	488	264	65	0	27	8	44	3	2	2	2	1	1	1
3	377	291	59	0	7	6	14	1	1	1	2	1	0	1
4	383	274	44	0	42	4	19	3	2	1	2	1	0	1
5	214	132	26	0	9	0	47	2	1	1	1	1	0	0
6	303	90	31	3	34	0	145	3	2	2	3	2	0	1
7	231	98	47	1	1	5	79	3	2	1	2	1	0	1
8	246	38	51	6	0	4	147	2	1	1	1	1	0	0
9	223	64	34	0	4	9	112	2	2	2	2	2	0	0
10	178	50	24	0	38	5	61	4	3	3	3	2	0	1
11	277	186	50	0	24	9	8	2	2	2	1	1	1	0
12	349	231	48	0	47	11	12	3	3	3	1	1	0	0
13	268	112	61	5	19	4	67	3	2	2	2	2	0	0
14	232	76	45	16	22	7	66	3	2	2	2	2	0	0
15	217	28	73	35	45	2	34	2	1	1	1	1	0	0
16	202	90	64	0	5	3	40	2	1	1	2	1	0	1
17	270	222	17	0	0	1	30	4	3	2	1	1	1	0
18	224	111	26	0	8	5	74	3	1	1	1	1	0	0
19	304	160	19	0	38	3	84	1	1	1	1	1	0	0
20	374	221	55	13	26	6	53	1	1	1	1	1	0	0
21	126	56	16	9	1	6	38	3	2	2	2	2	0	0
22	311	176	47	0	6	7	75	7	5	3	1	1	1	0
23	326	182	64	5	6	2	67	3	1	1	1	1	0	0
24	213	52	67	18	0	3	73	5	4	2	1	1	1	0
25	58	42	16	0	0	0	0	0	0	0	1	0	0	1

Table 2. Results of Green Citrus Recognition

Illumination condition	Fruit count	Correctly identified(%)	False positives(%)	Missed(%)
GCDRGF(sunny, both sides)	122	100(81.97%)	15(13.04%)	22(18.03%)
GCDRGF(sunny, sunny side)	67	55(82.09%)	7(11.29%)	12(17.91%)
GCDRGF(sunny, shadow side)	55	45(81.82%)	8(15.09%)	10(18.18%)
GCDRGF(cloudy)	77	61(79.22%)	17(21.8%)	16(20.78%)
GCDRGF(mixed, cloudy and sunny)	199	161(80.9%)	32(16.58%)	38(19.1%)
Eigenfruit[13](sunny, both sides)	122	92(75.41%)	41(30.83%)	30(24.59%)
Eigenfruit[13](sunny, sunny side)	67	50(74.63%)	31(38.27%)	17(25.37%)
Eigenfruit[13](sunny, shadow side)	55	42(76.36%)	10(19.23%)	13(23.64%)

4. Conclusions

In this study, we developed a novel green citrus fruit detection algorithm based on the proposed reticulate grayladder feature. A majority voting method was designed to utilize the statistical charecteristics of retuculate grayladder feature and apparent features of fruit regions to detect the target fruits. Both the qualitative and quantitative experimental results proved the effectiveness of the proposed algorithm. Compared with existed eigenfruit algorithm, GCDRGF had a higher rate of successful recognition and a lower rate of false positives.

The main advantage of the algorithm is the proposed reticulate grayladder feature, which represents the graylevel shift(statistical characteristics) of fruits' surface instead of color features and is independent of illumination changes, making the algorithm more suitable for the detection of green citrus fruits.

The perfomance of the algorithm can be also improved when it is combined with other methods, such as edge detection operators, spatial context and other useful cues.

Acknowledgments

This study is funded by the zhejiang provincial natural science foundation (LY17F030006, LQ15E050004), National Natural Science Foundation of China (61203327, 31471419), National High-tech R&D Program of China (863Program, No. 2013AA102307) and Ningbo city natural science foundation (2014A610079, 2015A610126).

References

[1] S. Sengupta and W. S. Lee, "Identification and determination of the number of immature green citrus fruit in a canopy under different ambient light conditions", Biosystems Engineering, vol. 117, **(2014)**, pp. 51-61.
[2] J. Cai, X. Zhou and Y. Li, "Recognition of mature oranges in natural scene based on machine vision", Nongye Gongcheng Xuebao/Transactions of the Chinese Society of Agricultural Engineering, vol. 24, no. 1, **(2008)**,pp. 175-178.
[3] Q. Yang, C. Liu and Y. Xun, "Target recognition for grape bagging robot", Nongye Jixie Xuebao/Transactions of the Chinese Society for Agricultural Machinery, vol. 44, no. 8, **(2013)**, pp. 234-239.
[4] Y. Cui, S. Su and X. Wang, "Recognition and feature extraction of kiwifruit in natural environment based on machine vision", Nongye Jixie Xuebao/Transactions of the Chinese Society for Agricultural Machinery, vol. 44, no. 5, **(2013)**, pp. 247-252.

[5] J. Yin, H. Mao and X. Wang, "Automatic segmentation method for multi-tomato images under various growth conditions", Nongye Gongcheng Xuebao/Transactions of the Chinese Society of Agricultural Engineering, vol. 22, no. 10, **(2006)**, pp. 149-153.
[6] A. R. Jiménez, R. Ceres and J. L. Pons, "A survey of computer vision methods for locating fruit on trees", Transactions of the American Society of Agricultural Engineers, vol. 43, no. 6, **(2000)**,pp. 1911-1920.
[7] P. Li, S. H. Lee and H. Y. Hsu, "Review on fruit harvesting method for potential use of automatic fruit harvesting systems", Procedia Engineering, **(2011)**, pp. 351-366.
[8] R. Chinchuluun and W. S. Lee, "Citrus yield mapping system in natural outdoor scenes using the watershed transform", Citrus yield mapping system in natural outdoor scenes using the watershed transform, 2006.
[9] K. E. Kane and W. S. Lee, "Multispectral imaging for in-field green citrus identification", In ASABE Paper no. 073025, **(2007)**.
[10] H. Okamoto and W. S. Lee, "Green citrus detection using hyperspectral imaging", Computers and Electronics in Agriculture, vol. 66, no. 2, **(2009)**, pp. 201-208.
[11] D. Stajnko, M. Lakota and M. Hočevar, "Estimation of number and diameter of apple fruits in an orchard during the growing season by thermal imaging", Computers and Electronics in Agriculture, vol. 42 no. 1, **(2004)**, pp. 31-42.
[12] E. E. Kelman and R. Linker, "Vision-based localisation of mature apples in tree images using convexity", Biosystems Engineering, vol. 118, no. 1, **(2014)**, pp. 174-185.
[13] F. Kurtulmus, W. S. Lee and A. Vardar, "Green citrus detection using 'eigenfruit', color and circular Gabor texture features under natural outdoor conditions", Computers and Electronics in Agriculture, vol. 78 no. 2, **(2011)**, pp. 140-149.
[14] Y. Si and G. Liu, "Gao, R. Segmentation algorithm for green apples recognition based on k-means algorithm", Nongye Jixie Xuebao/Transactions of the Chinese Society of Agricultural Machinery, vol. 40, supp. 1, **(2009)**, pp. 100-104.
[15] R. Linker, O. Cohen and A. Naor, "Determination of the number of green apples in RGB images recorded in orchards", Computers and Electronics in Agriculture, vol. 81, **(2012)**, pp. 45-57.
[16] C. M. Bishop, "Pattern recognition and machine learning", Springer: **(2006)**.
[17] J. Lu and N. Sang, "Detection of citrus fruits within tree canopy and recovery of occlusion contour in variable illumination", Nongye Jixie Xuebao/Transactions of the Chinese Society for Agricultural Machinery, vol. 45, no. 4, **(2014)**, pp. 76-81+60.

Author

Mingjun Wang, received his PhD degree at Mechatronics Institute, Shanghai Jiaotong University, China, in 2010. His research interests include machine vision, agricultural robots and pattern recognition.

